Printing Gold Nanoparticles with an Electrohydrodynamic Direct-Write Device

S.R. Samarasinghe*, Isabel Pastoriza-Santos$, M.J. Edirisinghe*=, M.J. Reece⁰ and Luis M. Liz-Marzán$

*Department of Mechanical Engineering, University College of London, Torrington Place, London, WC1E 7JE, UK

⁰Department of Materials, Queen Mary, University of London, Mile End Road, London, E1 4NS, UK

$Department of Physical Chemistry, University of Vigo, Vigo 36310, Spain

Abstract

A dispersion containing 15nm gold particles in ethanol was subjected to electrohydrodynamic atomization, producing droplets with an average size of ~26μm as measured by laser diffraction. An electrohydrodynamic direct-write device was used to deposit the dispersion onto silicon wafers with the intention of printing gold tracks. Immediately after deposition ethanol evaporated, leaving the gold particles organised in a ~75μm wide central region surrounded by two regions, each ~50μm wide, at the edge of which two further gold tracks, each ~7μm existed.

Keywords

nanoparticles, nano-suspensions, printing, direct writing, patterning, electrohydrodynamic, atomization

= Corresponding author: m.edirisinghe@ucl.ac.uk

Introduction

Gold and gold alloys are important functional materials (1-3). Gold has been a mainstay in the semiconductor and electronics industry with applications such as high temperature monitoring circuits in aerospace, automotive applications (2) and microwave electronic fabrication (3). However, as the demand for electronic, photonic and bio-electronics technology rapidly increases, the utilization of gold and its alloys will be thoroughly scrutinized, particularly in terms of cost and efficiency. Current gold track depositing techniques are ink-jet printing, electron-beam or laser driven and tend to use organometallic precursors (2, 4, 5). The cost, yield and purity of such routes are of concern and motivated us to use a gold colloid to direct-write gold tracks in a more economical way.

Direct write using ink-jet printing is known as the prime technique for depositing and patterning functional materials in the liquid phase onto a substrate (6). Modified ink-jet methods such as laser cured ink-jet technology (7) can generate microdroplets in the range of 60 – 100μm. However, as demonstrated in the traditional piezo-head technology based ink-jet printing of a gold track (8), it is well known that in ink-jet printing the droplets generated are larger than the nozzle's diameter and even if a fine (65μm diameter) ink-jet nozzle is used, the deposited droplet relics are well over a 100μm in diameter. In contrast, the electrohydrodynamic process allows much coarser nozzles (200-500μm in internal diameter) to be used, yet droplet and deposited droplet relics of less than 50μm can be achieved (9,10).

The electrohydrodynamic process usually consists of two electrodes, the first being a nozzle (needle) below which a second electrode (usually grounded) is held. The second electrode can be a ring, a plate or a point. An electric field is applied between the needle and the ground electrode while a suspension flows at a controlled rate through the needle. The surface of the flowing medium is subjected to an electrical stress and deforms locally to form an elongated jet, which subsequently evicts from the body of liquid, basically when the electric field is high enough to overcome the surface tension. The jet disintegrates into droplets. The geometry of jetting is classified into different modes of spraying (11,12) and it is well known that the stable cone-jet mode makes it possible to regularise the break-up of the jet to generate droplets of tens of micrometers in size, which are also highly uniform in size. A ring or plate shaped second electrode allows the droplets to diverse and is useful in the preparation of nano-sized and other powders (13,14) and coatings and films (15,16) but, in contrast the use of a pointed second electrode helps to focus the droplets and direct write (17). Furthermore using a lower flow rate and higher applied voltage produces smaller droplets (18) and this helps to minimize the size of printed lines.

In this paper, we report our initial findings on the electrohydrodynamic deposition of a very dilute gold alcosol

and the resulting track formation. A more extensive study on different alcosols and the assessment of track properties achieved is underway.

Experimental

Preparation of gold alcosol

Tetrachloroauric acid ($HAuCl_4.3H_2O$) and trisodium citrate were purchased from Aldrich. Poly(vinylpyrrolidone) (PVP, MW 10,000) was supplied by Fluka. All chemicals were used as received. Milli-Q water was used to make up all solutions (R > 18.2 Ω mm).

Gold nanoparticles with an average diameter of around 15 nm and 10% polydispersity were synthesized according to the standard sodium citrate reduction method (19) by boiling 5 x 10^{-4} M $HAuCl_4$ in the presence of 1.6 x 10^{-3} M sodium citrate for 15 min. After cooling down, the particles were transferred into ethanol upon functionalization with PVP (20). Briefly, an amount of PVP sufficient to coat the particles with 60 PVP monomers per nm^2 surface was dissolved by ultrasonication for 15 min in water and added to the gold colloid. The polymer was allowed to adsorb to the gold particles overnight while stirring. The particles were subsequently centrifuged (3500 r.p.m.) to remove the unbound PVP and redispersed in ethanol which was used as the liquid carrier as with our previous work on electrohydrodynamic materials processing. The final gold colloidal dispersion contained 0.1 wt % gold particles.

Electrohydrodynamic studies

The equipment used (Figure 1a) consisted of a stainless steel needle with internal and external orifice diameters of ~200μm and ~400μm, respectively, and held in epoxy resin. The needle was connected to a high voltage power supply (Glassman Europe Ltd., Tadley, UK) and the applied voltage was raised gradually to 5kV with respect to the ground electrode, which was a pointed rod. The inlet of the needle was connected to a Harvard PHD 4400 programmable syringe pump (HARVARD Apparatus Ltd., Edenbridge, UK) using a silicone rubber tube, and the flow rate of suspension to the needle exit was varied between 10^{-10} – 10^{-11} m^3s^{-1}. A fibre optic light source was used for illumination. A microscope lens in conjunction with a high speed camera (Weinberger AG, Dietikon, Switzerland), which was connected to a portable computer, allowed observation of the colloid while undergoing atomization.
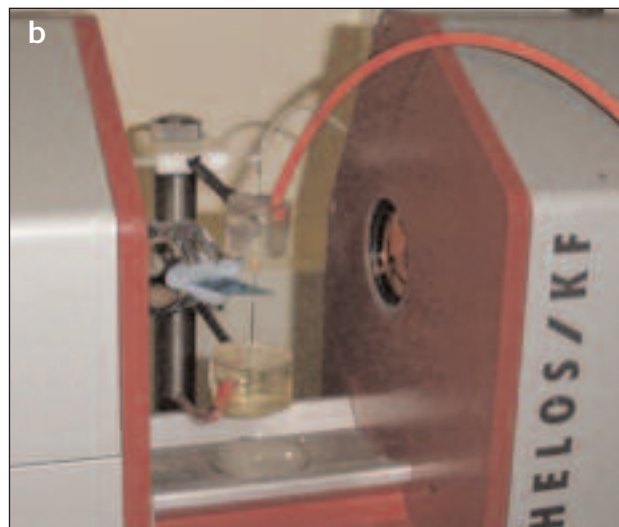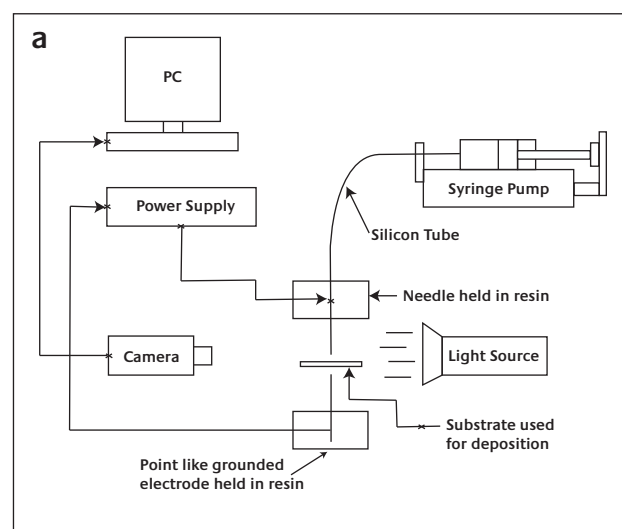
Droplet sizing

The droplet size distributions resulting from the atomization of the alcosol were measured using a model KF Sympatec helium laser optical spectrometer sizing system (Sympatec

Ltd., System Partikel-Technik, Bury, UK) in conjunction with a computer for recording and plotting of data as in our previous work (21,22). The laser system was incorporated in the electrohydrodynamic atomization equipment by placing it so that the 2.2mm diameter laser beam was approximately just below the exit of the needle in order to try and simulate the direct writing experimental conditions given below (Figure 1b).

Direct writing

The device used consists of a stepper motor driven 2D system. The X and Y tables are mounted on one another keeping the 2-axis profile very low and the system is computer-controlled using a programmable motion controller. A datum and an end of travel limit sensor are fitted on each of the tables to trigger the controller when a respective carriage reaches a limit. A Perspex table is mounted firmly on the 2-axis system. The top of the table accommodates a frame for holding firmly up to an A4 sheet

Figure 1

Equipment set-up used in: (a) electrohydrodynamic experiments (b) droplet size measurement

of substrate. Using motion planner software X and Y coordinates can be created and downloaded to the 2-axis controller, allowing the 2-axis system to write the path described by the coordinates provided.

After the 2-axis system was set-up, the needle and point were aligned. Subsequently, the substrate, a silicon wafer, was placed ~0.4mm below the needle. The silicon wafer used was boron doped P-type, 525μm thick and having a 400nm SiO_2 layer on both sides. Throughout writing the grounded point electrode was kept at a distance of ~4mm below the substrate. A potential difference was applied between the needle and the point while the suspension was pumped through the needle at a pre-determined flow rate. The equipment used in this part of the process was identical to those used in electrohydrodynamic experiments described above.

The printed tracks were dried for 24 hours at room temperature and coated with carbon before examination by scanning electron microscopy and energy dispersive X-ray analysis. The SEM characterization was carried out with a JEOL JSM-6700F FEG-SEM operating at an acceleration voltage of 15 kV in lower secondary electron image (LEI) and at 10 kV in backscattering electron image (YAG). The elemental analysis was performed with an Oxford INCA Energy 300 X-ray Energy Dispersive Spectrometer (EDS) system.

Results and discussion

The alcosol is very stable and no sedimentation occurred on standing for several days. For classical electrohydrodynamic atomization (EHDA) to occur, the hydrodynamic time (t_h) must exceed the electrical relaxation time (t_e), and the inequality $\frac{LD^2}{Q} \gg \frac{\beta\epsilon_0}{K}$ must be satisfied (23). L denotes the axial length of the jet, D is the jet diameter, Q is the flow rate, K is the electrical conductivity and β is the relative permittivity. ϵ_0 is the permittivity constant and is 8.85x10^{-12} Fm^{-1}.
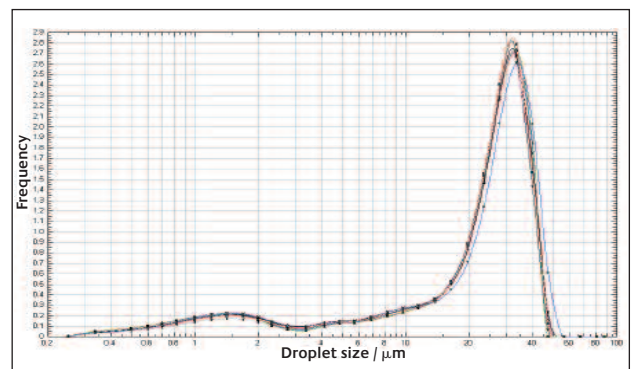
In our electrohydrodynamic experiments, the flow rate (Q) and applied voltage were kept constant at 5 x 10^{-11} m^{3}s^{-1} and 4.8 kV, respectively, as these conditions generated a stable cone-jet (Figure 2), which is well known to produce a monodisperse stream of fine droplets. D and L measured were ~15μm and ~325μm, respectively, giving an electrohydrodynamic time of 1.46 x 10^{-3} s. Using the β and K values of ethanol as 26 and 3.4 x 10^{-4} Sm^{-1}, respectively (24) t_e is 6.77 x 10^{-7} s. Thus $t_h \gg t_e$ and the condition required for classical EHDA is satisfied. The 0.1 wt. % of gold can only make the K value even higher to satisfy this inequality even more comfortably, but a high K value can impose an upper limit on the flow rate (25).

High applied voltages and lower flow rates are beneficial to print finer tracks as explained earlier. However, in general, increase of applied voltage resulted in discharge and at lower flow rates a stable cone-jet could not be maintained. Also the
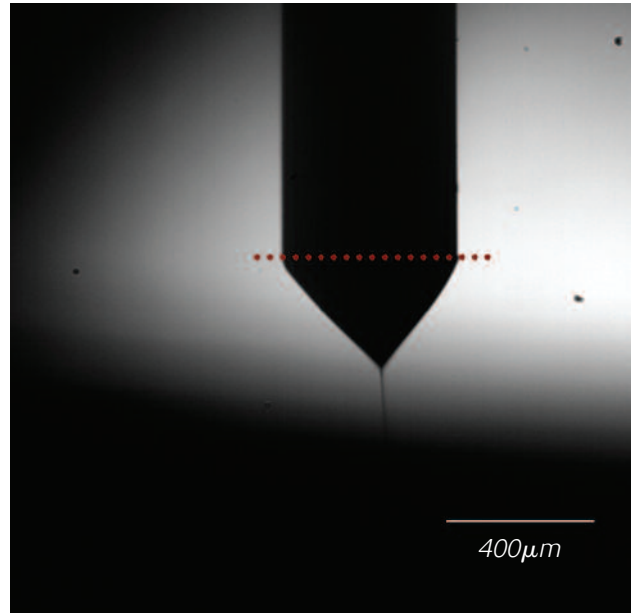
Figure 2
Stable cone-jet mode of electrohydrodynamic atomization of the gold alcosol at 4.8kV and 5 x 10^{-11} m^{3}s^{-1}. Exit of the needle is indicated with a dotted line

Figure 3
Typical droplet size distribution obtained by electrohydrodynamic atomization of the gold alcosol. Duplicate plots refer to repeated experiments

distance between the needle and the substrate was selected as 0.4mm and the distance between the substrate and the ground electrode was set at 4mm because they gave the finest line width without scattering of the droplet relics. When the distance between the substrate and needle, substrate and ground electrode was increased it produced a significant amount of scattering and when the distance was decreased, a stable cone-jet was not achieved.

The droplets generated by the cone-jet was in the range of 0.25μm - 60μm (Figure 3). The average droplet size was ~26μm and the standard deviation was 5.7μm. Different track geometries were prepared (Figures 4a and b) and the finest gold track deposited was ~110μm wide. However, immediately after deposition, the gold nano-particles organised into narrow sub-tracks (Figure 5a). The typical width of the middle track was ~75μm and the tracks at the boundary were ~7μm. Energy dispersive x-ray analysis confirmed that these regions of the original printed tracks

Table 1

A summary of results from investigations attempting the forming of conductive tracks. Parenthesis indicates the references

| Method	Solution	Particle size	Metal (wt. %)	Minimum Track Size
Chemical e-Beam Lithography (27)	Citrate-passivated gold nanoparticles	16nm	-	100nm
Fountain Pen (28)	Gold nanoparticles in toluene	2-4nm	30	5μm
Micro-contact electroless plating technique (29)	Gold nanoparticles in colloid solution	3nm	-	5μm
Laser direct write (30)	Gold Ink	-	-	8μm
Ink-jet Printing (7)	Gold nanoparticles in toluene	2-5nm	30	15μm
Ink-jet Printing (31)	Gold nanoparticles in toluene	2-4nm	30	20μm
Ink-jet Printing (32)	Gold nanoparticles in toluene	5-20nm	30-50	100μm
Ink-jet Printing (33)	Gold nanoparticles in toluene	2-4nm	30	125μm
Ink-jet Printing (34)	Silver nanoparticles in α-terpineol	5-7nm	10	100μm
Ink-jet Printing (35)	Silver nanoparticles in toluene	1-10nm	30	120μm
Ink-jet Printing (36)	Silver ink in xylene	-	16	160μm
Ink-jet Printing (37)	Silver nanodispersion	50nm	8	1.5mm
Microcontact Printing (38)	Copper	-	-	500nm
Chemical Vapor Deposition (39)	Copper	-	-	1μm
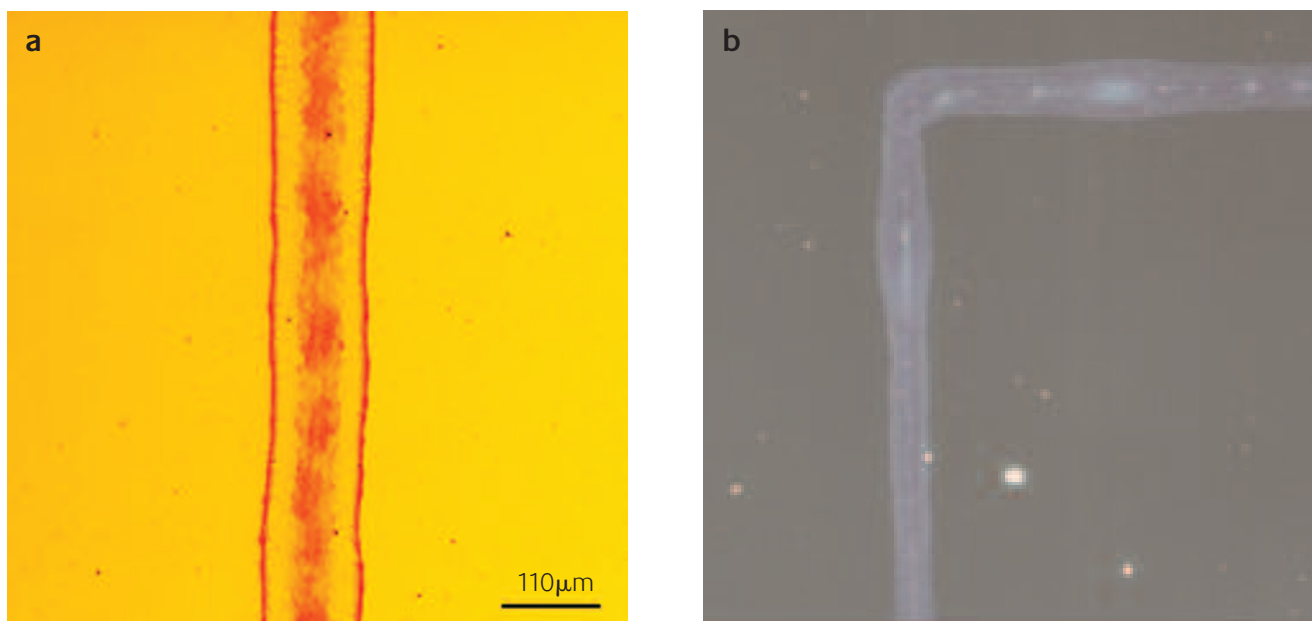
Figure 4

Micrographs of different tracks produced using the direct write device: (a) the flow rate was set to 5 x 10^{-11} m^3s^{-1} and applied voltage was 4.8 kV; and (b) the flow rate was 9.17 x 10^{-11} m^3s^{-11} and applied voltage was 4.1kV. The track width in (b) is ~ 350μm

contained the nano-gold particles. A similar kind of particle arrangement has been reported by Cuk et al. (26) in their work with copper particles, and their flow visualization studies identified Bénard–Marangoni convection as the mechanism responsible for formation of multiple lines from a single printed track.

Figure 5 (b) shows a high-resolution SEM image of the edge of the track and Figures 5(c) and (d) shows similar images of the central track where most of the nano-gold particles assemble. From Figure 5(d) it is clear that a considerable proportion of the gold particles are not densely packed, hence leaving voids between particles and obviously this type of particle arrangement is not ideal for producing electrically conducting gold tracks.

The ability to direct write metallic lines < 20μm and having the electrical conductivity of its bulk material would open up a whole new realm of possibilities (1). Table 1 shows the different reported methods used for producing conductive tracks, ink-jet printing is the prime technique, and a minimum track size of about 15μm (7) has been achieved after coupling laser technology with ink-jet printing and using a suspension having a gold particle concentration of 300 times than that used in the present work. Experiments using more concentrated metal colloids are underway with the objective of electrohydrodynamic deposition of even finer conductive tracks.
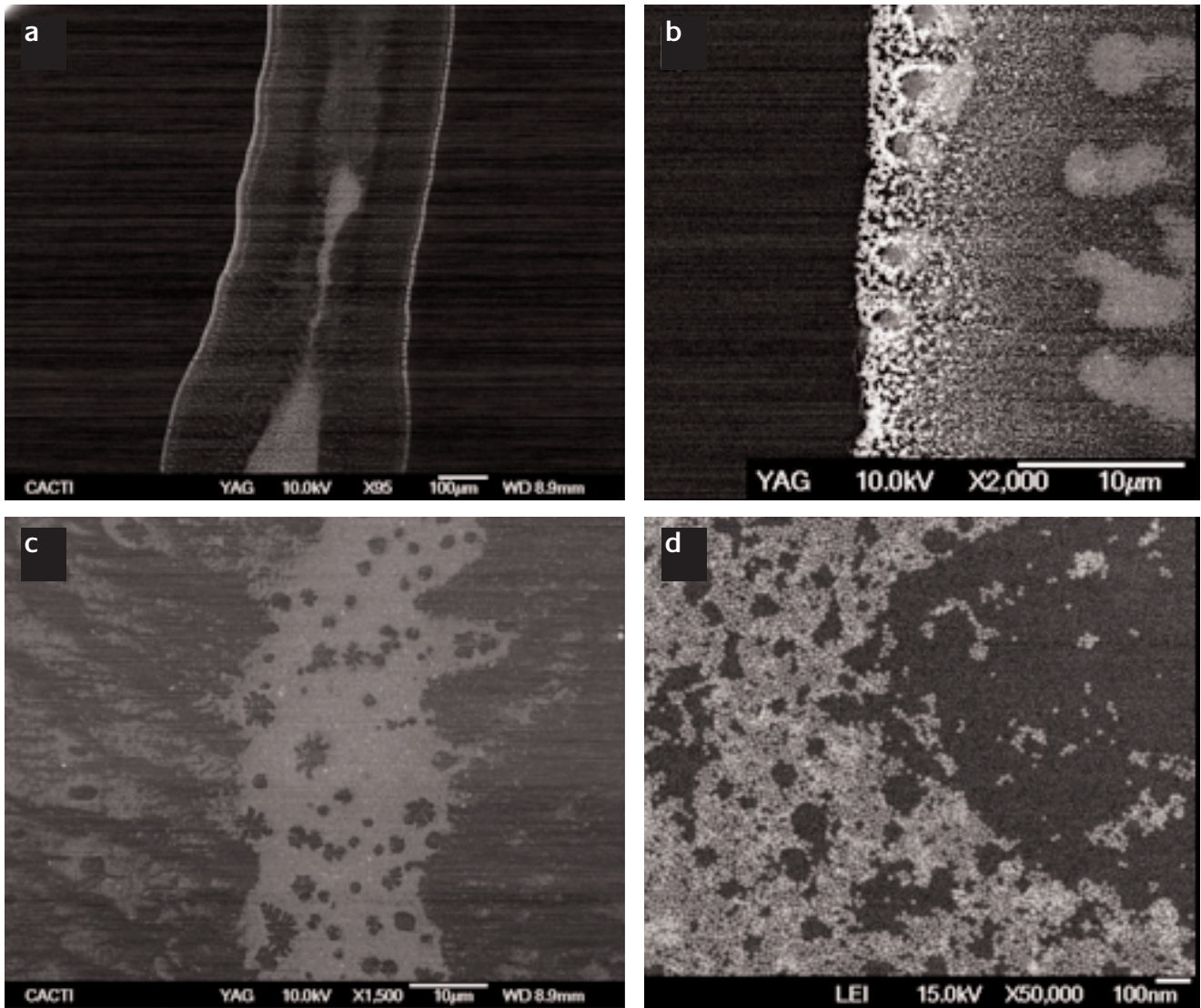
Figure 5
Scanning electron micrographs of the printed track: (a) whole track; (b) an edge track; (c) and (d) centre track

Conclusions

A gold nano-suspension has been subjected to an electrohydrodynamic process and the droplets generated have been deposited using a 2D patterning device in an attempt to directly write metal tracks. Due to the Bénard−Marangoni effect gold particles organize into three lines, having a narrow width compared with the original printed track and do not form continuous gold tracks. We anticipate that the use of a more concentrated suspension may be helpful in this regard, however varying the shape of the gold particles could also improve connectivity and this is also being investigated.

References

1   T.W. Ellis, *Gold Bulletin*, 2004, **37**, 66

2   J.R. Greenwood, P.R.N. Childs and P. Chaloner, *Gold Bulletin,* 1999, **32**, 85

3   G. Humpston, *Gold Bulletin*, 1999, **32**, 75

4   G.J. Berry, J.A. Cairns and J. Thomson, *Sensors & Actuators A,* 1995, **51**, 47

5   D. Tonneau, J.E. Bouree, A. Correia, G. Roche, G. Pelous and S. Verdeyme, *J. Appl.Phys.,* 1995, **78**, 5139

6   H. Sirringhaus and T. Shimoda, *MRS Bulletin,* 2003, **28**, 802

7   N.R. Bieri, J. Chung, D. Poulikakos and C.P. Grigoropoulos, *Superlattice Microst.*, 2004, **35**, 437

8   H.M. Nur, J.H. Song, J.R.G. Evans and M.J. Edirisinghe, *J. Mater.Sci. − Mater. In Electr.,* 1999, **13**, 213

9   S.N. Jayasinghe and M.J. Edirisinghe, *Appl. Phys. A.,* 2005, **80**,701

10 D.Z. Wang, S.N. Jayasinghe and M.J. Edirisinghe, *J. Nanopart. Res.,* 2005, **7**, 301

11 A. Jaworek and A. Krupa, *J. Aerosol Sci.,* 1999, **30**, 873

12 M. Cloupeau and B. Prunet-foch, *J. Aerosol Sci.*, 1994, **25**, 1143

13 S.N. Jayasinghe, R. Dorey, M.J. Edirisinghe and Z. Luklinska, *Appl. Phys. A.*, 2005, **80**, 723

14 D.A. Grigoriev, M.J. Edirisinghe and X. Bao, *J.Mater. Res.*, 2002, **17**, 487

15 B. Su and K.L. Choy, *Thin Solid Films*, 2002, **361**, 102

16 S.N. Jayasinghe and M.J. Edirisinghe, *J .Mater. Sci. Lett.*, 2003, **22**, 1617

17 S.N. Jayasinghe, M.J. Edirisinghe and T. De Wilde, *Mater. Res. Innovat.*, 2002, **6**, 92

18 S.N. Jayasinghe and M.J. Edirisinghe, *J. Euro. Ceram. Soc.*, 2004, **24**, 2203

19 B.V. Enustun and J. Turkevich, *J. Am. Chem. Soc.*, 1693, **85**, 3317

20 C. Graf, D.L.J. Vossen, A. Imhof, and A.V. Blaaderen, *Langmuir*, 2003, **19**, 6693

21 S.N. Jayasinghe and M.J. Edirisinghe, *J. Appl. Ceram. Tech.*, 2004, **1**, 140

22 S.N. Jayasinghe, M.J. Edirisinghe and D.Z. Wang, *Nanotechnology*, 2004, **15**, 1519

23 A.M. Ganan-Calvo, J. Davila and S. Barrero, *J. Aerosol Sci.*, 1997, **28**, 249

24 D.Z. Wang, S.N. Jayasinghe and M.J. Edirisinghe, *Rev. Sci. Instr.*, 2005, **76**, 075105

25 F. Schulz, S. Franzka and G. Schmid, *Adv. Functional Mater.*, 2002, **12**, 532

26 T. Cuk, S.M. Troian, C.M. Hong and S. Wagner, *Appl. Phys. Lett.*, 2005, **77**, 2063

27 P.M. Mendes, S. Jacke, K. Critchley, J. Plaza, Y. Chen, K. Nikitin, R.E Palmer, J.A. Preece, S.D. Evans and D. Fitzmaurice, *Langmuir*, 2004, **20**, 3766

28 T.Y. Choi, D. Poulikakos and C.P. Grigoropoulos, *Appl. Phys. Lett.*, 2004, **85**, 13

29 F. Guan, M.A. Chen, W. Yang, J.Q. Wang, S.R. Yong and Q.J. Xue, *Appl. Surf. Sci.*, 2005, **240**, 24

30 S. Corbett, J. Strole and K. Johnston, *Applied Ceramic Technology*, 2005, **2**, 390

31 N.R. Bieri, J. Chung, S.E. Haferl, D. Poulikakos and C.P. Grigoropoulos, *Appl. Phys. Lett.*, 2004, **82**, 3529

32 J.B. Szczech, C.M. Megaridis, J. Zhang and D.R. Gamota, *Microscale Therm. Eng.*, 2004, **8**, 327

33 J. Chung, S. Ko, N.R. Bieri, C.P. Grigoropoulos and D. Poulikakos, *Appl. Phys. Lett.*, 2004, **84**, 801

34 S.B. Fuller, E.J. Wilhelm and J.A. Jacobson, *J. Microelectromech S.*, 2002, **11**, 54

35 J.B. Szczech, C.M. Megaridis, D.R. Gamota and J. Zhang, *IEEE Transactions on Electronics Packaging Manufacturing*, 2002, **25**, 26

36 A.L. Dearden, P.J. Smith, D.Y. Shin, N. Reis, B. Derby and P. O'Brien, *Macromol. Rapid Comm.*, 2005, **26**, 315

37 A. Kamyshny, M. Ben-moshe, S. Aviezer and S. Magdassi, *Macromol Rapid Comm.*, 2004, **26**, 281

38 P.C. Hidber, W. Helbig, E. Kim and G.M. Whitesides, *Langmuir*, 1996, **12**, 1375

39 S.J. Potochnik, P.E. Pehrsson, D.S.Y. Hsu and J.M. Calvert, *Langmuir*, 1995, **11**, 1841